Geocarto International

ISSN: 1010-6049 (Print) 1752-0762 (Online) Journal homepage: http://www.tandfonline.com/loi/tgei20

Image quality characterization of fine resolution RISAT-1 data using impulse response function

Gautam Dadhich, Shweta Sharma, Mihir Rambhia, Aloke K. Mathur, P. R. Patel & Alpana Shukla

To cite this article: Gautam Dadhich, Shweta Sharma, Mihir Rambhia, Aloke K. Mathur, P. R. Patel & Alpana Shukla (2018): Image quality characterization of fine resolution RISAT-1 data using impulse response function, Geocarto International, DOI: 10.1080/10106049.2017.1421715

To link to this article: https://doi.org/10.1080/10106049.2017.1421715

Accepted author version posted online: 26 Dec 2017.
Published online: 08 Jan 2018.

GEOCARTO INTERNATIONAL, 2018
https://doi.org/10.1080/10106049.2017.1421715

Taylor & Francis
Taylor & Francis Group

Image quality characterization of fine resolution RISAT-1 data using impulse response function

Gautam Dadhich[a], Shweta Sharma[b], Mihir Rambhia[c], Aloke K. Mathur[b], P. R. Patel[a] and Alpana Shukla[d]

[a]Civil Engineering Department, Nirma University, Ahmedabad, India; [b]Calibration and Validation Division, Space Applications Centre, ISRO, Ahmedabad, India; [c]Department of Civil, Geo and Environmental Engineering, TUM, Munich, Germany; [d]Botany Department, M.G. Science Institute, Ahmedabad, India

ABSTRACT

This study presents the results obtained from image quality assessment of Radar Imaging SATellite (RISAT-1). Image quality parameters such as spatial resolution, peak to sidelobe ratio (PSLR) and integrated sidelobe ratio (ISLR) are calculated by the analysis of impulse response function (IRF) of the point target. The study is carried out to assess temporal stability and consistency of image quality parameters obtained from analysis of IRF of 44 point targets. The results obtained from this study show that the mean values of the range and azimuth resolution are 2.048 ± 0.081 m and 3.383 ± 0.097 m for RH and 1.981 ± 0.081 m and 3.348 ± 0.076 m for RV, respectively. PSLR/ISLR values for RH channel are obtained as −26.492 dB/−26.823 dB for azimuth and −19.209 dB/−19.921 dB for the range. For RV channel, PSLR/ISLR values are −26.300 dB/−27.572 dB for azimuth and −19.146 dB/−19.827 dB for range.

ARTICLE HISTORY
Received 16 May 2017
Accepted 15 December 2017

KEYWORDS
SAR; PSLR; ISLR; RISAT-1; image quality; corner reflector; impulse response function

1. Introduction

The Radar Imaging SATellite -1 (RISAT-1) is India's indigenous space-borne SAR C-band sensor functioning since 2012. RISAT-1 synthetic aperture radar uses 126 beams to generate full range of defined image products. RISAT-1 has imaging capabilities in Stripmap and ScanSAR modes with resolution from 1 to 50 m and swath coverage from 25 km to 223 km, with multi-polarization capabilities along with hybrid circular polarimetric mode (Misra et al. 2013; Misra and Kirankumar 2014). RISAT-1 is operating in scanSAR, strip and spot modes to provide images with coarse, fine and high spatial resolutions, respectively. Detailed specifications of RISAT-1 SAR beam modes are given in Table 1 (Misra et al. 2013).

In order to maintain the given image quality from the RISAT-1 system requirement, the monitoring of the image quality is needed throughout the operational phase. The quality of SAR image is affected by system variables because SAR image passes through complicated processes such as synchronization of centre frequency, bandwidth and antenna power, unlike an optical image. The SAR image quality depends on spatial resolution, PSLR and ISLR of point target response. These

CONTACT Gautam Dadhich gautamdadhich3392@gmail.com

Table 1. Basic design/operating parameters of the RISAT-1 radar.

Parameters	Values
Centre frequency	5.35 GHz ± 112.5 MHz
Antenna dimensions	6 m (along flight) × 2 m (cross flight)
Antenna beam width	0.5° × 1.5°
Gain	44.5 dB
Gain bandwidth	1.0 dB
Panel size	2 m × 2 m
Chirp type	I/Q baseband
Chirp Bandwidth	75 MHz
Sampling rate	83.3 MHz
PRF (Hz)	3000 ± 200
Pulse width	20/10 µs

image quality parameters can be obtained by modelling Impulse Response Function (IRF) from point target response in SAR data. The SAR response to a point target, with the assumption of negligible clutter backscattering and noise, is stated as IRF (Freeman 1992). The quality measurements using IRF usually need corner reflectors deployment. In addition to monitoring of image quality, IRF is also used to validate digital image processing algorithms. Yang et al. 2015 proposed two dimensional SAR algorithms for phase error compensation and direct digital synthesizer (DDS)-based chirp signal generator. The proposed algorithm (Yang et al. 2015) was validated using PSLR and ISLR obtained from IRF. Spatial resolution is the most significant parameter for image quality assessment as compared to PSLR and ISLR. The spreading energy of the main lobe over sidelobes is indicated by ISLR (Vu 2011). PSLR deals with sensors' capability to image response of less intensity target affected by a high-intensity target nearby (Das 2011). Image quality assessment studies using IRF of point target for SAR on board KOMPSAT-5 (Li et al. 2015), RADARSAT-1 (Srivastava et al. 2007) and RISAT -1 (Rajesh et al. 2015) satellites proved the validity of this method of measurement of image quality.

Annual monitoring of SAR image quality on different beams and polarizations for FRS data of RISAT-1 is required to ensure the consistency, stability and validity of quality parameters. To evaluate the image quality parameters, the impulse response of reflectors in both range and azimuth directions is measured. Initial image quality assessment of RISAT-1 data was carried out by Gupta et al. 2014 and it was concluded that the image quality parameters were within the limit and well consistent. In order to maintain image quality as per system requirement, it is important to study and monitor the quality parameters temporally. Hence, in this study, temporal stability assessment of image quality parameters is carried out. The newly developed calibration site is capable of providing better point target response which enables reliability of results.

2. Site for CR deployment

Suitable site selection for the point target deployment is the prime requirement. The suitable site should be selected based on flatness and homogeneity of the surrounding land, perceived sources of radar clutter in the vicinity, distance from metallic boundary fences and overlap of adjacent point target (CR) responses (Garthwaite et al. 2015). For this study, the site was selected in Despair, Rann of Kutch, Gujarat, which meets all above-mentioned criteria. The site is located at central latitude and longitude of 23°46′14.10″ N and 70°43′19.30″ E as shown in Figure 1. The selected site is comprised of homogenous areas of 03.00 × 07.00 m with uniform soil. The point targets were deployed at particular locations within the area where background reflection is less as compared to point target response. The fact that the site is devoid of any buildings and vegetation and its large

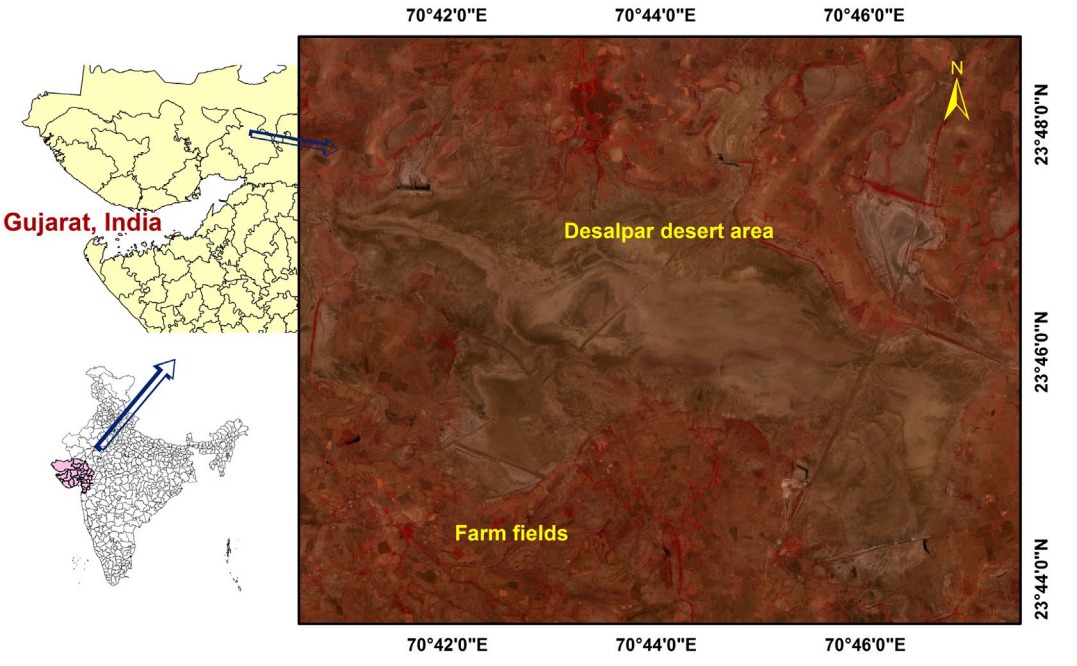

Figure 1. Calibration site at Desalpar, Rann of Kutch. Source: Sharma et al. 2017).

uniform area make this site a potential site for the calibration of high and medium resolution SAR sensors. Figure 2 shows corner reflector of 0.9 m leg length (Length of CR Panel) with adjustable wooden mount at calibration site, which shows background scene of corner reflector.

3. Methodology

For each corner reflector, the image quality parameters viz. spatial resolution, PSLR and ISLR are determined. In this study, triangular trihedral corner reflector of 0.90 m leg length is deployed at Desalpar, Kutch, Gujarat (India) on March 2016 (beam no. 107), 11th March (beam no. 87) and April 2016 (beam no. 108). Desalpar, Rann of Kutch (Gujarat) having homogeneous background bare soil in desert environment site was used as site for corner reflector (CR) deployment. Corner reflectors are deployed on the site with a minimum spacing of 600 m between two corner reflectors. Total seven CRs on 10 and 11 March and eight CRs on 29 April are deployed. The location, azimuth and elevation angle of the corner reflectors used in the study are shown in Table 2. For corner reflectors' (CRs) response analysis, circular polarization images, i.e. RH (right-hand circularly polarized transmit and linearly receive in horizontal polarization) and RV (right-hand circularly polarized transmit and linearly receive in vertical polarization), were used in the present study. The image quality parameters are determined within same scene having seven/eight corner reflectors. IRF of 44 point targets (22 RH/22 RV) are generated by point target analysis and same clutter (32/16 pixels) and point target (8 pixels) window sizes are kept to ensure the applicability of the final results. Intensity images from un-calibrated Level-1 FRS-1 data are generated using commercially available gamma software package (Warner et al. 2000) for both RH and RV polarization. The location of CR is interpreted based on the response of the deployed corner reflector in the intensity image. The point target analysis is carried out to generate IRF. Figure 3 shows the representative IRF of an isolated point target. The IRF is a sinc function with a clutter of the main lobe and many secondary lobes. The figure shows a 2-D section of the typical IRF in the azimuth direction. The peak intensity is the maximum pixel value in the main lobe of the

Figure 2. Corner reflector at calibration site, Desalpar, Rann of Kutch.

Table 2. Location, azimuth and elevation angle of the corner reflectors used in the study.

Date	Location	CR No	Latitude Deg.	Min.	Sec.	Longitude Deg.	Min.	Sec.	Azimuth (°)	Elevation angle (°)	Remarks
10 and 11 March, 2016	Desalpar, Kutch, India	CR1	23	45	57.8	70	43	3.2	280.43	16.59	Descending pass Left look East facing CRs
		CR2	23	46	29.4	70	42	6.8			
		CR3	23	46	50.2	70	41	36.2			
		CR4	23	46	26.1	70	43	32.4			
		CR5	23	46	6.4	70	43	50			
		CR6	23	46	43.2	70	43	1.9			
		CR7	23	46	52.1	70	42	35.7			
29 April, 2016		CR1	23	45	58	70	43	0.8	260.27	7.40	Ascending pass Left look West facing CRs
		CR2	23	46	29.2	70	42	8.1			
		CR3	23	46	51.5	70	41	33.3			
		CR4	23	46	31	70	43	17.5			
		CR5	23	46	12.3	70	43	45.4			
		CR6	23	46	59.3	70	42	54.7			
		CR7	23	47	0.1	70	43	16.6			
		CR8	23	46	57	70	43	34.1			

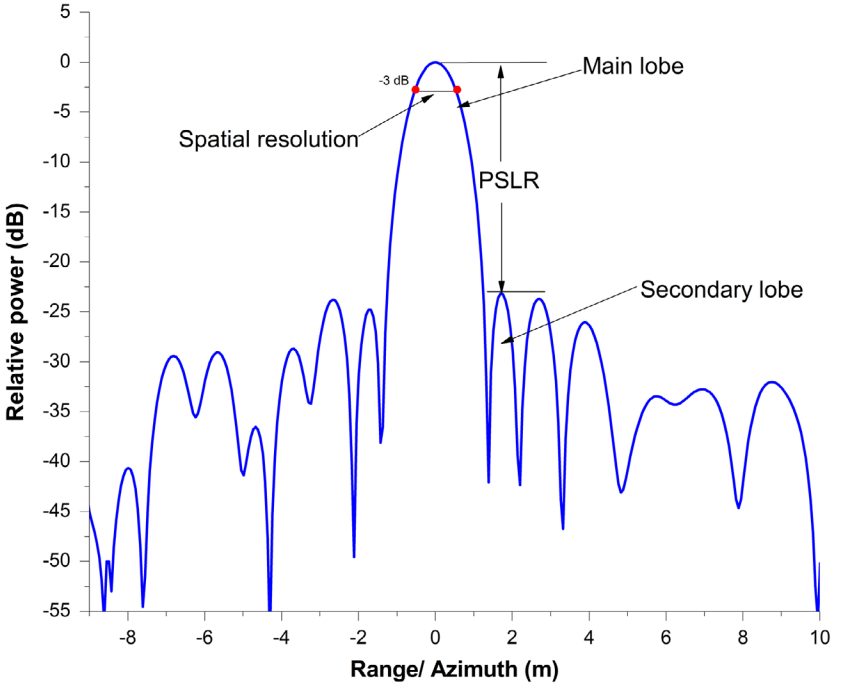

Figure 3. Typical IRF of an SAR point target depicting various image quality parameters (Martinezl and Marchand 1993).

IRF. The spatial resolution is the −3 dB width of peak lobe. The methodology used to estimate spatial resolution, PSLR and ISLR for fine resolution RISAT data is presented in Figure 4.

The spatial resolution is defined as the distance between two objects on the ground surface at which the images of the objects can be seen distinct and separate (Zénere 2012). From the IRF, spatial resolution can be calculated as the distance between two points at −3 dB of main lobe as shown in Figure 3 of IRF which are 3 dB below the peak lobe.

The peak sidelobe ratio, PSLR, is referred as the ratio of the peak intensity of the most intense side lobe to the peak intensity of the main lobe of IRF. There are two measures of the PSLR, corresponding to the two sides of the main lobe both in azimuth and range directions. The PSLR is calculated by Equation 1 as per Committee on Earth Observing System (CEOS) standards (CEOS, 1989).

$$\mathrm{PSLR} = 10\log_{10}\frac{I_s}{I_m} \tag{1}$$

where 'I_s' stands for the peak intensity of the most intense side lobe and 'I_m' stands for the peak intensity of the main lobe.

The integrated sidelobe ratio (ISLR) is the ratio of the energy in the main lobe to the cumulative power in all the side lobes of clutter window. It presents the ability to detect weak target's response in the neighbourhood of highly reflective targets and is a measurement of the relative reflectance of the side lobes on the main lobe (Vu et al. 2008). In this study, ISLR is determined by modified European Space Agency (ESA) method (ESA 1991) as shown in Equation 2.

$$\mathrm{ISLR} = 10\log_{10}\frac{\int_{10\times10}\mathrm{Idxdy} - \int_{2\times2}\mathrm{Idxdy}}{\int_{2\times2}\mathrm{Idxdy}} \tag{2}$$

4. Results and discussion

RISAT-1 FRS-1 data products acquired on 10 March, 11 March and 29 April 2016 have been used for IRF analysis. Results of image quality parameters obtained from the IRF measurements for SAR

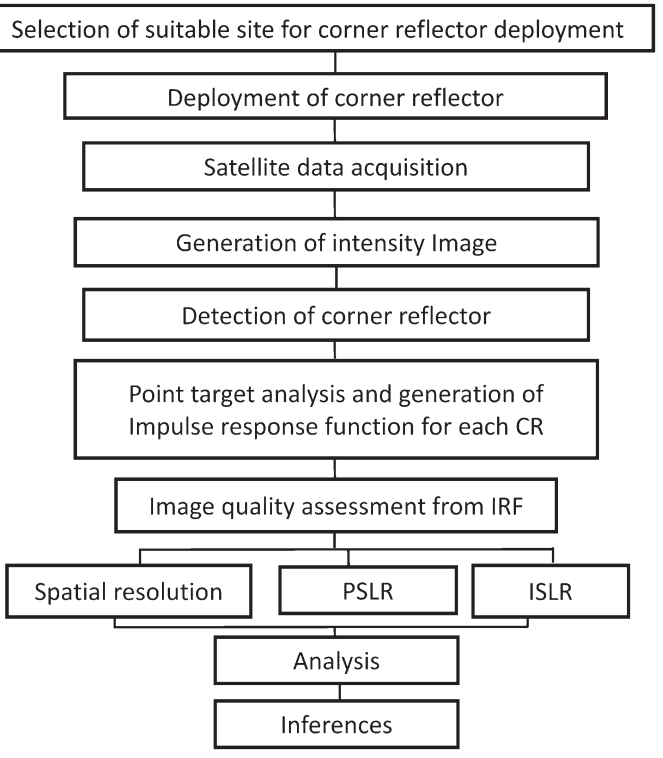

Figure 4. Methodology adopted for image quality assessment.

data are discussed in this section. The calculations are performed on the image interpolated by sinc interpolation. The quality of SAR image has been assessed from IRF measurements of a point target. The typical response of CRs in the SAR image of 10 March 2016 satellite pass and the location of seven point targets are shown in the Figure 5. The locations of the corner reflectors are shown in Figure 5. Bright point targets response of 0.9 m TTCR is clearly seen in the SAR image. IRF analysis

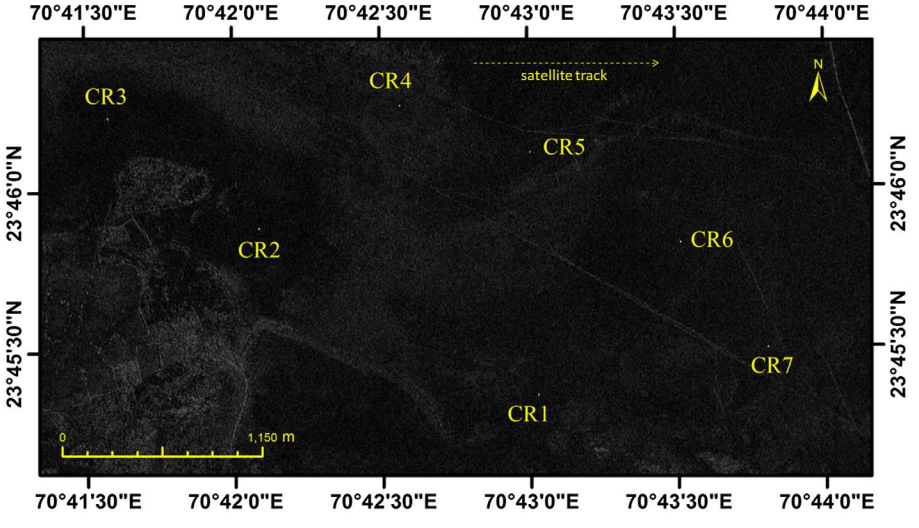

Figure 5. 10 March 2016 FRS-1 Image (RH Polarization).

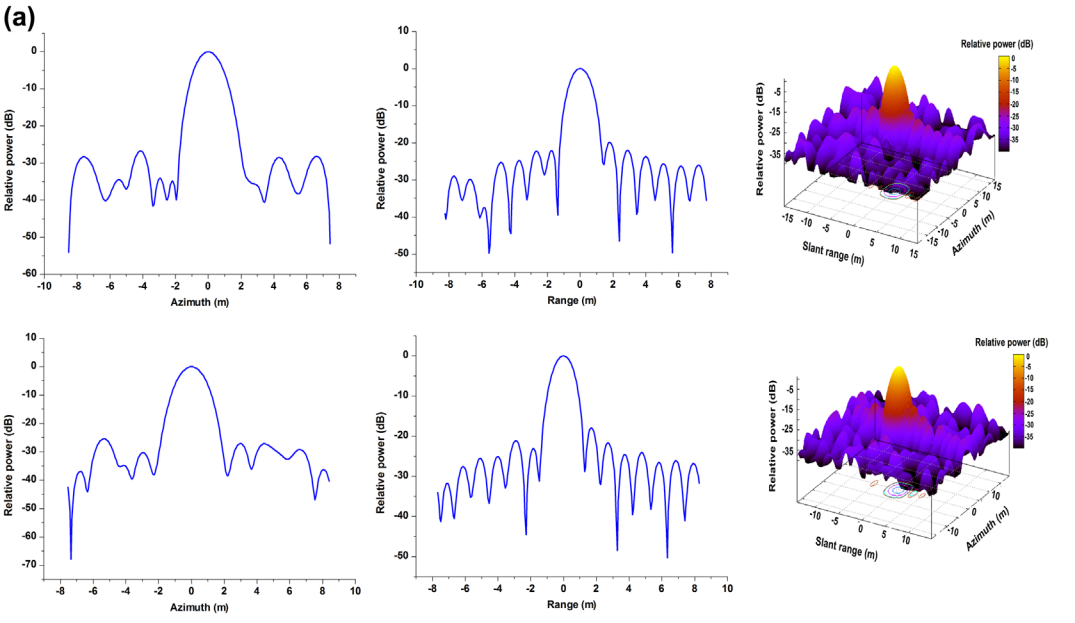

Figure 6a. Typical IRF results of 10 March 2016 in RH (above) and RV (Below) polarization.

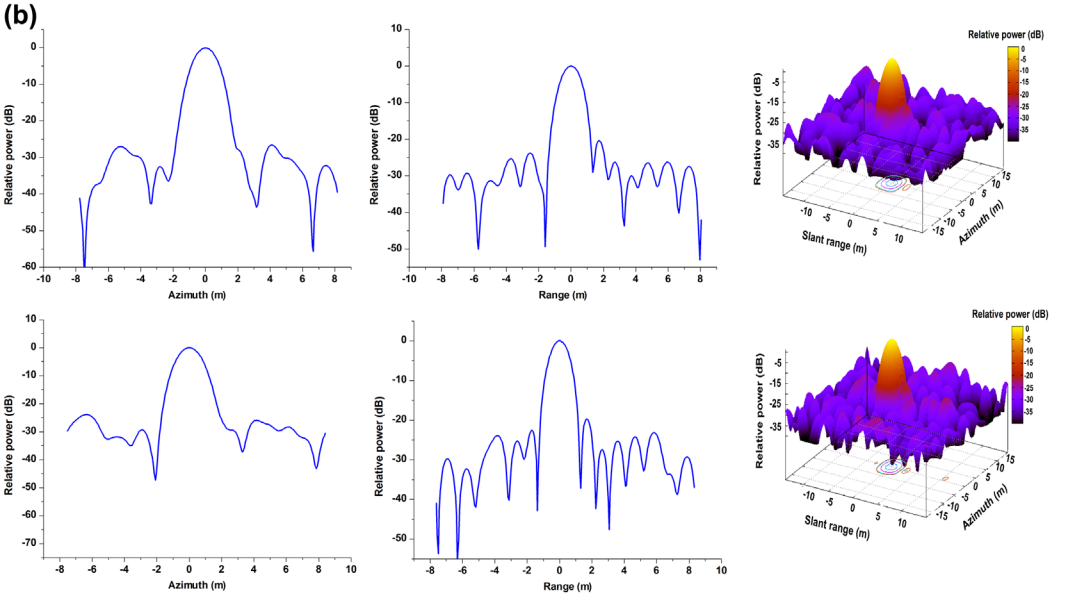

Figure 6b. Typical IRF results of 11 March 2016 in RH (above) and RV (Below) polarization.

was carried out by the methodology described in Figure 4 to generate IRF for each point target for all of the acquired images. The IRF of point target is obtained by applying Integral method (Gray et al. 1990). To obtain the reliable results, same clutter and point target window size are kept. Figure 6 shows the two-dimensional section of IRF, relative power (dB) on ordinate and background width on abscissa along with a three-dimensional view of IRF of acquired data. These IRF were used to estimate the image quality parameters. To derive more accurate image quality parameters, IRF was generated

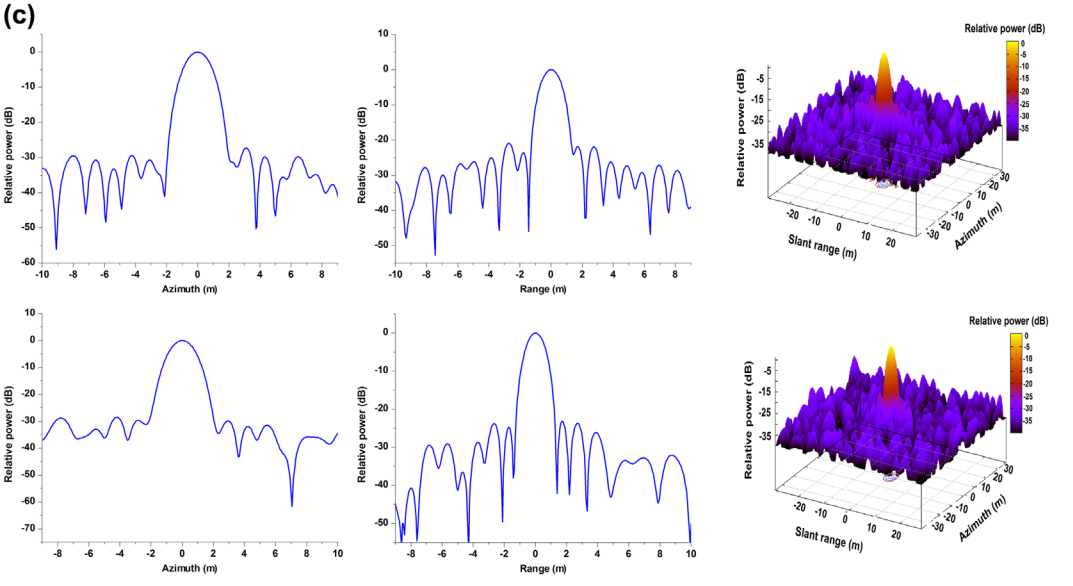

Figure 6c. Typical IRF results of 29 April 2016 in RH (above) and RV (Below) polarization.

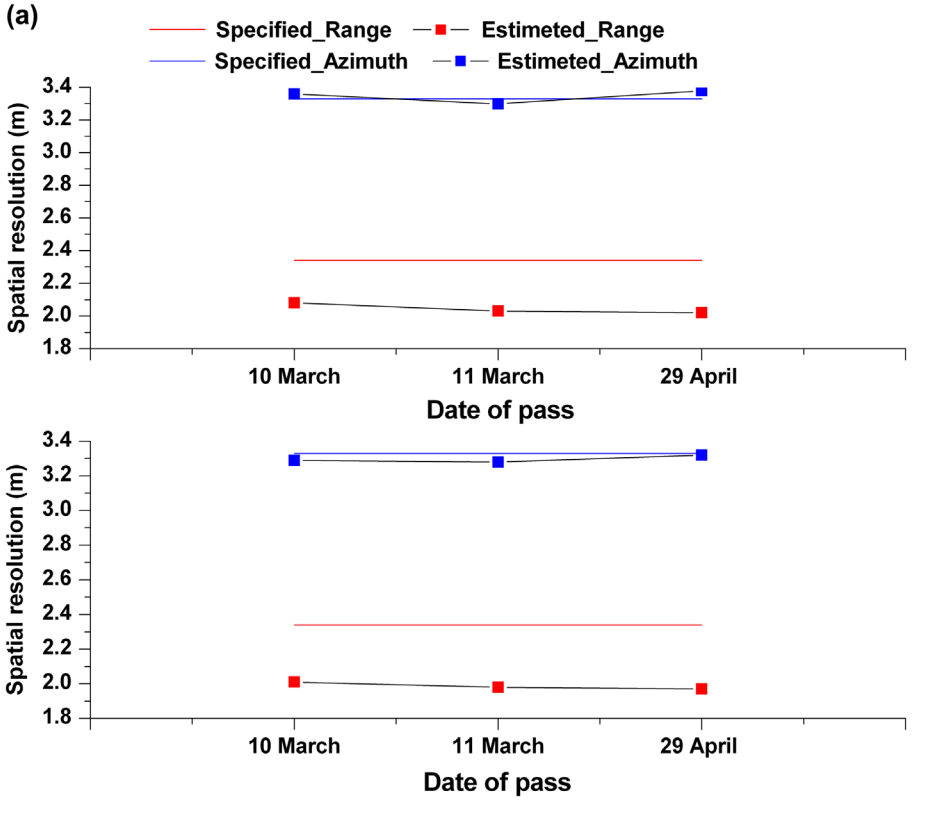

Figure 7a. Temporal variation of spatial resolution for RH (above) and RV (Below) polarization.

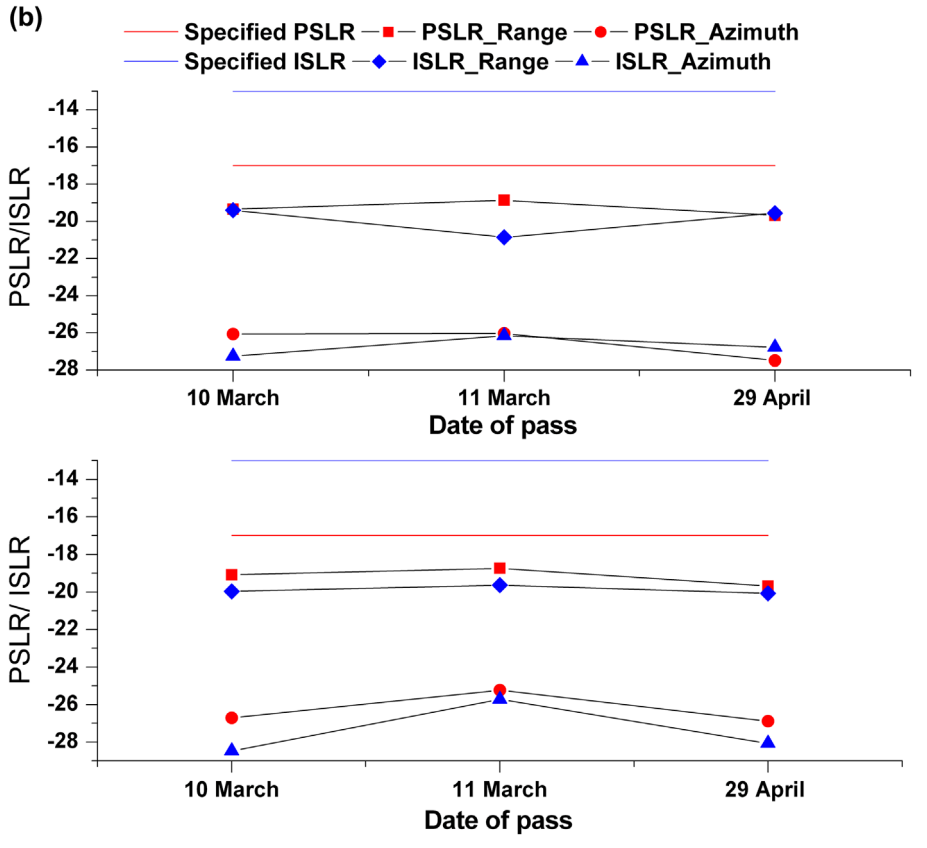

Figure 7b. Temporal variation of estimated PSLR and ISLR for RH (above) and RV (Below) polarization.

Table 3. Statistical results of the estimated image quality parameters.

Polarization		Range resolution (m)	Azimuth resolution (m)	Range PSLR (dB)	Azimuth PSLR (dB)	Range ISLR (dB)	Azimuth ISLR (dB)
RH	Mean	2.048	3.383	−19.209	−26.492	−19.921	−26.823
	St. Dev.	0.081	0.097	1.609	3.146	2.107	3.126
	Max.	2.166	3.454	−14.815	−19.925	−17.318	−20.952
	Min.	1.88	3.106	−22.285	−32.97	−27.946	−36.15
RV	Mean	1.981	3.348	−19.146	−26.3	−19.827	−27.572
	St. Dev.	0.081	0.763	1.674	1.962	1.409	2.637
	Max.	2.166	3.454	−16.711	−23.158	−16.999	−22.716
	Min.	1.88	0.097	−22.147	−31.24	−21.837	−32.198

on interpolated image. The signature of point target and sidelobes clearly shows that corner reflectors were deployed at uniform background having negligible reflectivity. In addition to this, shape of IRF signature is also not distorted, which ultimately proves reliability and accuracy of estimated image quality parameters.

The temporal results of image quality parameters obtained using IRF of CRs are shown in Figure 7(a). It shows the temporal variation of estimated spatial resolution for RH and RV polarization, respectively. The specified value of range resolution is 2.34 m, and azimuth resolution is 3.33 m for FRS-1 data, which is provided in system specification for RISAT-1 sensor (NRSC 2015). The figure

shows that the estimated values of spatial resolution in both range and azimuth are well consistent with time and as per the system specification for both RH and RV polarization.

The temporal variation of estimated PSLR and ISLR for RH and RV polarization for FRS-1 data PSLR/ISLR estimated using IRF of CRs is shown in Figure 7(b). RISAT-1 data product-specified values of PLSR and ISLR are −17 and −13 dB, respectively. Graphical results show that the estimated values of PSLR and ISLR in range and azimuth are well consistent with time and within the specified values (−17 dB (PSLR) and −13 dB (ISLR)). It is clearly seen in the figure that PSLR and ISLR in azimuth direction are better than the specified values. Similar results are also reported for other RISAT-1 data products (Rajesh et al. 2015).

The statistical results obtained from analysis of IRF of 44 (22RH/ 22RV) point targets, image quality parameters are presented in Table 3. From the IRF of the deployed CRs, the obtained mean of azimuth resolution (3.38 ± 0.097 m for RH and 3.34 ± 0.076 m for RV) is almost similar to value provided in mission specification (3.33 m). The mean value of range resolution obtained (2.04 ± 0.08 m for RH and 1.98 ± 0.081 m for RV) from IRF is better than the specified value (2.34 m). On the other hand, it is observed that PSLR and ISLR are quite lower than the expected value for both RH and RV channel. The reason behind these higher sidelobe ratio's is less reflective, smooth and superior signal to clutter ratio (>20 dB). The estimated results of image quality parameters obtained from IRF of point target are within limit and well consistent with the specified value. These results depict that image quality of the RISAT-1 image of the FRS-1 mode is well temporally stable and improvement has been seen on the range and azimuth resolution.

5. Conclusion

Image quality evaluation of RISAT-1 SLC Level-1 FRS-1 data is carried out using IRF generated from triangular trihedral corner reflector of 0.90 m leg length. The CRs are deployed at the newly developed calibration site at Desalpar, Kutch on 10 March, 11 March and 29 April 2016. Point target analysis is carried out by the integral method to generate IRF. Spatial resolution, PSLR, and ISLR, is determined from IRF of each date and each corner reflector. The estimated values of range resolution are better than the specified resolution, whereas the values of azimuth resolution are almost similar to the specified values. PSLR/ISLR values for RH channel are obtained as −26.492 dB/−26.823 dB for azimuth and −19.209 dB/−19.921 dB for the range. For RV channel, PSLR/ISLR values are −26.300 dB/−27.572 dB for azimuth and −19.146 dB/−19.827 dB for range. For RH channel, the range of estimated azimuth PSLR is found to be −32.97 to −19.92 and estimated azimuth ISLR ranges between −36.15 and −20.95. The range of estimated range PSLR is found to be −22.285 to −14.815 and estimated range ISLR ranges between −36.15 and −20.95 for RH channel. For RV channel, the range of estimated azimuth PSLR is found to be from −23.158 to −31.24 and estimated azimuth ISLR ranges between −22.716 and −32.198. The range of estimated range PSLR is found to be −16.711 to −22.147 and estimated range ISLR ranges between −16.999 and −21.837 for RH channel. It is observed that the mean of range resolution, ISLR; PSLR obtained from IRF is quite better than values of the FRS-1 system specification. This study proves that image quality of fine resolution data of RISAT-1 is satisfactory and sensor and data processing perform well since the launch of the satellite. Outcomes of this study are useful in the development of data processing methods for future SAR missions.

Acknowledgement

Authors express their sincere gratitude to Director, Space Applications Centre, Ahmedabad and Deputy Director, EPSA for their guidance and support to carry out this activity. Authors are grateful to Director, Institute of Technology, Nirma University, HOD, Civil Engineering Department, Nirma University and Principal, M.G. Science Institute, Ahmedabad for their institutional support for carrying out this activity. Authors also thankfully acknowledge the cooperation and technical help received from Shri R. P. Prajapati, Shri D. B. Dave, Dr. Kartikeyan, Shri Ramanujam, Shri Amit Shukla and Shri Raghav Mehra for this activity. The help and support rendered by Shri Ganuba, Shri Digvijay and Shri Parvat

during the deployment of Corner reflectors at Desalpar and their geographical guidance of the local area were of utmost importance for the successful calibration campaigns.

Disclosure statement

No potential conflict of interest was reported by the authors.

Funding

This work is supported by our own organization Space Applications Centre, ISRO, Ahmedabad.

References

Anonymus. 1991. ESA, ECISAR TEST IMAGE: quality analysis and calibrations measurements.
Das SK. 2011. Synthetic Aperture Radar image quality measurements [dissertation]. Karlskrona: Blekinge Institute of Technology.
Freeman A. 1992. SAR calibration: an overview. IEEE Trans Geosci Remote Sens. 30(6):1107–1121. DOI:10.1109/36.193786.
Garthwaite MC, Nancarrow S, Hislop A, Thankappan M, Dawson JH, Lawrie S. 2015. Design of radar corner reflectors for the Australian Geophysical Observing System. Geosci Aust. 3:7–28.
Gray AL Vachon PW, Livingstone CE, Lukowski TI. 1990. Synthetic Aperture Radar Calibration Using Reference Reflectors. IEEE Trans Geosci Remote Sens. 28(3):374–383. 10.1109/36.54363
Gupta M, Sharma A, Kartikeyan B. 2014. Image quality assessment of RISAT-1 SAR using trihedral corner reflectors in different beams. J Geomatics. 8(2):130–139.
Li CR, Tang LL, Ma LL, Zhou YS, Gao CX, Wang N, Li XH, Wang XH, Zhu XH. 2015. Comprehensive calibration and validation site for information remote sensing. Int Arch Photogrammetry, Remote Sens Spatial Info Sci. 40(7):1233. [10.5194/isprsarchives-XL-7-W3-1233-2015]
Martinezl A, Marchand J. 1993. SAR image quality assessment. Revista de Teledeteccion. 2:12–18.
Misra T, Rana SS, Desai NM, Dave DB, Rajeevjyoti, Arora RK, Rao CVN, Bakori BV, Neelakantan R, Vachchani JG. 2013. Synthetic Aperture Radar payload on-board RISAT-1: configuration, technology and performance. Curr Sci. 104(4):446.
Misra T, Kirankumar AS, 2014. RISAT-1: configuration and performance evaluation. In General Assembly and Scientific Symposium (URSI GASS), 2014 XXXIth URSI, Aug 16–23; Beijing. p. 1–4.
NRSC 2015. RISAT-1 data products format Retrieved from www.nrsc.gov.in/sites/all/pdf/format3.pdf.
Rajesh J, Ponnurangam GG, Kumar V, Rao YS, Ramanujam VM. 2015. Calibration of RISAT-1 compact polarimetric SAR system using point targets. CEOS Calibration and Validation Workshop 2015-ESA-Noordwijk; The Netherlands.
SAR Data Products Format Standard – WGISS – CEOS. 1989. [accessed 2017 Apr 4]. wgiss.ceos.org/archive/archive.pdf/sardata.pdf.
Sharma S, Dadhich G, Rambhia M, Mathur AK, Prajapati RP, Patel PR, Shukla A. 2017. Radiometric calibration stability assessment for the RISAT-1 SAR sensor using a deployed point target array at the Desalpar site, Rann of Kutch, India. Int J Remote Sens. 38(23):7242–7259. DOI: 10.1080/01431161.2017.1371858.
Srivastava SK, Cote S, Le Dantec P, Hawkins RK, Murnaghan K. 2007. RADARSAT-1 calibration and image quality evolution to the extended mission. Adv Space Res. 39(1):7–12.[10.1109/IGARSS.2004.1368632]
Vu VT. 2011. Ultra Wideband-Ultra wide beam Synthetic Aperture Radar–Signal Processing and Applications [dissertation]. Blekinge Institute of Technology.
Vu VT, Sjögren TK, Pettersson MI, Gustavsson A. 2008. Definition on SAR image quality measurements for UWB SAR. Proc SPIE Image Signal Process Remote Sens XIV. 7109:7109A. DOI:10.1117/12.799478]
Warner C, Wegmüller U, Strozzi T, Wiesmann A. 2000. Gamma SAR and Interferometric Processing Software. Proceedings of ERS-Envisat Symposium, Sweden. 1620:1620.
Yang li, Jing Zhnag, Chengbin Fu, Dalong W. 2015. BEMD based two dimensional SAR autofocus Algorithm. Geocarto Int. 30(10):1163–1171. DOI: 10.1080/10106049.2015.1034193
Zénere, MP. 2012. SAR image quality assessment. Cordoba: Universidad Nacional de Cordoba